

Monoslepton production in hadronic collisions

John M^cCurry¹

*Theory Group, Department of Physics,
University of Southampton,
Southampton SO9 5NH, ENGLAND*

ABSTRACT

Single sparticle creation in high energy collisions as a consequence explicit R -parity breaking, could be a rich source of highly spectacular signals at future colliders. One particular process, which could lead to a highly exotic leptonic signal at the LHC, is monoslepton production. In this paper we qualitatively discuss the constraints on the signal for this process and calculate the hadronic monoslepton production cross section, taking into account leading QCD corrections. Our results show the leading corrections could be quite significant at the proposed LHC operating energy.

¹E-mail: jmcc@hep.phys.soton.ac.uk

1 Introduction

It has been shown[1] that certain superstring theories possess natural discrete symmetries which allow R -parity breaking[2] but prevent unacceptably fast proton decay by excluding a subset of the possible R -parity breaking operators from the superpotential. Low energy supersymmetric models naturally arising out of such theories admit an acceptable phenomenology and thus appear as plausible as the MSSM. Such R_p -broken models therefore deserve to be confronted with a degree of experimental interest commensurate with that being directed towards searching for the MSSM. In minimal R_p -broken models the most general allowed renormalizable superpotential has the form

$$W = W_{\text{MSSM}} + W_{\mathcal{R}_p}, \quad (1.1)$$

where W_{MSSM} is the usual mass generating superpotential of the MSSM, and

$$W_{\mathcal{R}_p} = \lambda_{ijk} L_i L_j \bar{e}_k + \begin{cases} \lambda'_{ijk} L_i Q_j \bar{d}_k \\ \text{XOR} \\ \lambda''_{ijk} \bar{u}_i \bar{d}_j \bar{d}_k \end{cases} \quad (1.2)$$

The transformation properties of the matter multiplets under $SU(3)_C \times SU(2)_L \times U(1)_Y$ are listed in Table 1 below. In eq. (1.2) the ‘XOR’ (exclusive or), which is necessary to avoid ex-

Superfield	Quantum Numbers
L	(1, 2, -1)
\bar{e}	(1, 1, 2)
Q	(3, 2, 1/3)
\bar{u}	($\bar{3}$, 1, -4/3)
\bar{d}	($\bar{3}$, 1, 2/3)

Table 1: Quantum numbers of matter multiplets under $SU(3)_C \times SU(2)_L \times U(1)_Y$

tremely fast proton decay, is provided by the aforementioned stringy discrete symmetries[1]. $W_{\mathcal{R}_p}$ generates new lepton- and baryon-number violating Yukawa interactions which can lead to spectacular signals in high energy collisions[3]. In this paper we examine the novel possibility of monoslepton (or anti-slepton) production in hadron collisions induced by one of the $[L Q \bar{d}]_F$ operators. At tree level this process proceeds via the graph shown in Fig. 1, where i, j and k are flavour indices.

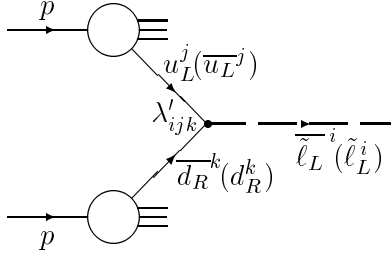


Figure 1: Single anti-slepton production at leading order.

If there is a dominant $[LQ\bar{d}]_F$ operator the tree level hadronic cross section has the form

$$\sigma_H^0 = K_0 \int_{\tau}^1 \frac{dx}{x} H(x, \tau/x). \quad (1.3)$$

Here $\tau = M^2/S$, $K_0 = \pi\lambda'^2/12S$, where M is the slepton mass, λ' is the Yukawa coupling of the dominant operator, and the hadronic CMS energy is \sqrt{S} . In order to extract any numerical results for the cross section it is necessary to invoke some assumptions about the flavour structure of the dominant operator. In this paper we shall assume that $\lambda' = \lambda'_{i11}$ ($i = 1, 2, 3$). Since the valence up quark content of the proton is greater than the valence down quark content, this particular flavour structure will favour anti-slepton production to slepton production. The parton kernel $H(x_1, x_2)$ for the dominant anti-slepton production mode is given in terms of the up and anti-down quark densities (u, \bar{d}) by

$$H(x_1, x_2) = u(x_1)\bar{d}(x_2) + u(x_2)\bar{d}(x_1). \quad (1.4)$$

Assuming $B(\tilde{\ell} \rightarrow \tilde{\gamma}\ell) \sim 1$ and that the photino is the LSP, the slepton/anti-slepton will decay to produce a dilepton and jets. The photino, being a Majorana fermion, can couple to both the \mathcal{R}_p operators and their charge conjugates which could allow the production of an unusual *isolated like-sign dilepton* (ILSD). Whether one or both leptons are isolated depends essentially on the photino to slepton mass ratio: $\rho = m_{\tilde{\gamma}}/m_{\tilde{\ell}}$. If the photino is very light (*i.e.* $\rho \ll 1$) the secondary lepton could be ‘lost’ in the hadronic shower and the signal would then appear to be a very energetic isolated lepton recoiling against a jet. However, assuming that the secondary lepton can be resolved some qualitative kinematic constraints on the dilepton are as follows:

1. Neglecting lepton masses, the energy of the primary lepton (l_1) is

$$E_1 = \frac{m_{\tilde{\ell}}}{2} (1 - \rho^2), \quad (1.5)$$

and $E_2 \in [\max(E_1 - m_{\tilde{\gamma}}/2, 0), E_1 + m_{\tilde{\gamma}}/2]$ for the secondary lepton (l_2).

2. For a moderately light photino (*i.e.* $\rho \leq (\sqrt{5}-1)/2 \approx 0.62$) the minimum kinematically allowed opening angle between the leptons is

$$\theta_{min}(\rho) = \pi - \sin^{-1} \left(\frac{\rho}{1 - \rho^2} \right) \in \left[\frac{\pi}{2}, \pi \right] \quad (1.6)$$

If $\rho > 0.62$ there is no constraint.

3. The missing transverse momentum carried by the leptons can be as large as $m_{\tilde{\gamma}}/2$.

Potentially large backgrounds from $t \rightarrow b W^+$ can be effectively excluded with a suitable cut on E_1 (*e.g.* $E_1 > O(m_t/2)$), whilst $q\bar{q}, H^0 \rightarrow W^+W^-$ can be eliminated on the basis of event topology (if the secondary lepton is isolated), or if necessary with $M_{\text{jets}} \neq O(M_W)$. A further cut $M_{l_1 l_2} \neq O(M_{Z^0})$ may be necessary to veto ‘fake’ energetic l^+l^- pairs from high- p_T Z^0 production giving an ILSD signal. In any case, after the standard model is removed monoslepton production at the LHC will have an exotic signature.

Turning our attention to the cross section we will now show that the leading QCD corrections to the tree level expression in eq. (1.3) are potentially large at proposed LHC energies (in fact $> 30\%$ for $M \gtrsim 1\text{TeV}$). Our calculation of these corrections closely follows the approach adopted by AEM (Altarelli, Ellis and Martinelli [4]) in their calculation of the leading QCD corrections to vector boson production. We, of course, extend the AEM calculation to consider additional one loop vertex and self energy corrections involving virtual squarks and gluinos.

2 The NLO corrections

2.1 Overview of calculation

The treatment of the NLO corrections to the total cross section is a straightforward perturbative calculation. The full $O(\alpha_s)$ contribution is obtained by adding the interference terms generated by the tree level diagram in Fig. 2 with the one loop diagrams in Fig. 3(a)-(d) to the sum of the ‘squares’ of the tree level diagrams in Fig. 4(a)-(d).

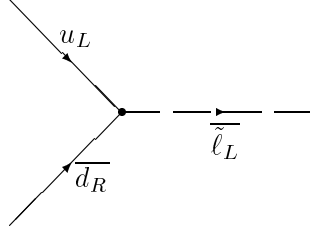


Figure 2: The leading order contribution to the elementary cross section

We evaluate the contribution from these diagrams as follows: Using dimensional regularisation to tackle both the UV and IR singularities we initially continue to $4 - 2\varepsilon$ dimensions ($\varepsilon > 0$) to address the UV divergences. Since IR divergences are manifest in $4 - 2\varepsilon$ dimensions we artificially ‘postpone’ the mass-singularity in the quark self energy by temporarily continuing external-line quarks off-shell. After renormalization of the UV divergences we then continue to $4 + 2\eta$ dimensions ($\eta > 0$) and return all external quarks on-shell. The IR divergences are now regularised and appear as single and double poles in η . The double poles, which originate from vanishingly soft virtual gluon emission/absorption processes, cancel when the contributions from the gluon bremsstrahlung and the one loop QCD diagrams are added. The single pole terms do not cancel completely, but those which survive (*i.e.* the ‘mass singularities’) are removed in the standard manner[4] by factoring them into the ‘bare’ NLO parton densities. We shall now briefly consider the contribution from the individual diagrams, starting with the loop diagrams.

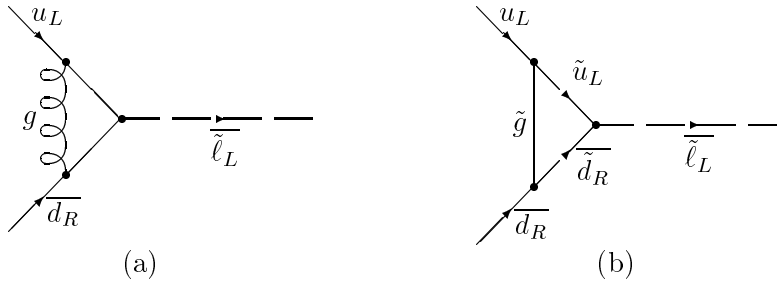


Figure 3(a),(b): The one-loop QCD and SSB vertex corrections

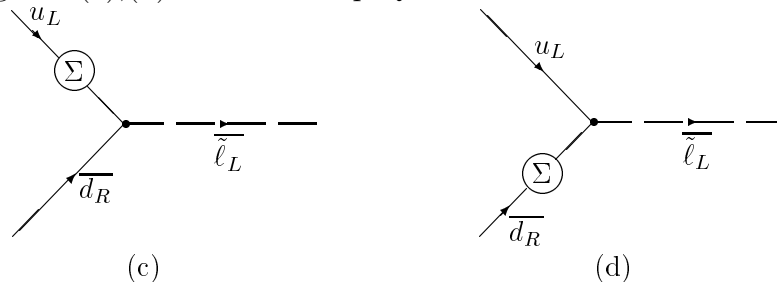


Figure 3(c),(d): The quark self-energy corrections ($\Sigma = \Sigma_{\text{QCD}} + \Sigma_{\text{SUSY}}$)

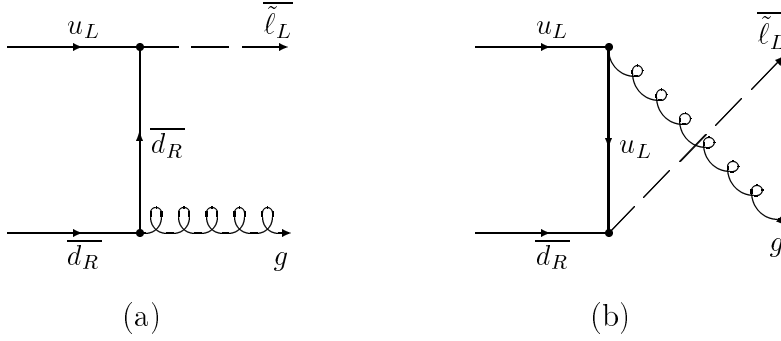


Figure 4(a),(b): The NLO ‘gluon bremsstrahlung’ corrections

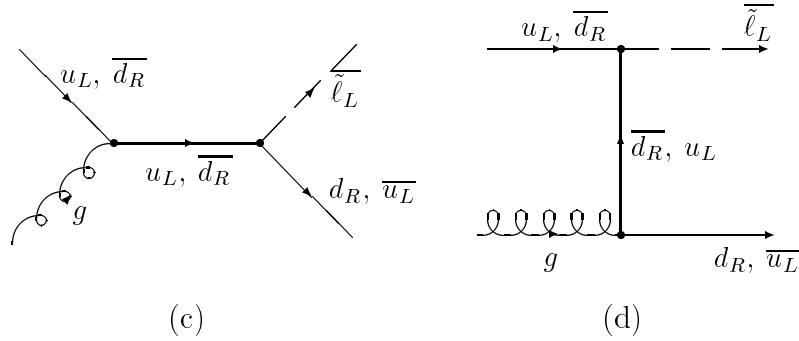


Figure 4(c),(d): The NLO ‘Compton scattering’ corrections

2.2 The one-loop contribution

The net effect of all of the loop diagrams (evaluated in $4 - 2\varepsilon$ dimensions) is to simply multiply the tree level cross section by a factor

$$1 + \frac{\alpha_s C_F}{\pi} L\left(\frac{1}{\varepsilon'}; \frac{1}{\varepsilon}, \frac{1}{\varepsilon^2}\right), \quad (2.1)$$

where α_s is the dimensionless strong coupling, C_F is the quadratic Casimir in the fundamental representation of the gauge group ($C_F = 4/3$ for $SU(3)$), and L is some function to be determined. Formally, $\varepsilon' = \varepsilon$ but the prime is used to indicate that the simple pole is of UV and not IR origin. Retaining only $O(\alpha_s)$ terms it is clear that we can re-write the multiplicative factor of (2.1) in the convenient factorised form

$$\left(1 + \frac{\alpha_s C_F}{\pi} L_{\text{UV}}\left(\frac{1}{\varepsilon'}\right)\right) \left(1 + \frac{\alpha_s C_F}{\pi} L_{\text{IR}}\left(\frac{1}{\varepsilon}, \frac{1}{\varepsilon^2}\right)\right) \quad (2.2)$$

where L_{UV} and L_{IR} contain the UV and IR poles respectively. Unfortunately, finite corrections ensure that L_{UV} and L_{IR} cannot be uniquely determined.

The QCD vertex correction

The overall effect of including the QCD vertex correction of Fig. 3(a) (calculated in the Feynman gauge) is to multiply the tree level cross section by the factor

$$1 + \frac{\alpha_s C_F}{2\pi} \left(\frac{\bar{\mu}^2}{M^2} \right)^\varepsilon \left(\frac{-2}{\varepsilon^2} + \frac{4}{\varepsilon'} - \frac{4}{\varepsilon} + \frac{7\pi^2}{6} - 2 + O(\varepsilon) \right). \quad (2.3)$$

Here M is the slepton mass, $\bar{\mu} = 4\pi\mu e^{-\gamma_E}$ where γ_E is the Euler-Mascheroni constant, and μ is an arbitrary scale introduced to ensure that α_s is always dimensionless:

$$\alpha_s = \frac{(\mu^2)^{-\varepsilon} g^2}{4\pi}. \quad (2.4)$$

For future convenience we will factor out the UV pole piece and re-write (2.3) in the ‘UV×IR’ form (neglecting $O(\alpha_s^2, \varepsilon)$):-

$$\left[1 + \frac{\alpha_s C_F}{2\pi} \left(\frac{\bar{\mu}^2}{M^2} \right)^\varepsilon \frac{4}{\varepsilon'} \right] \left[1 + \frac{\alpha_s C_F}{2\pi} \left(\frac{\bar{\mu}^2}{M^2} \right)^\varepsilon \left(\frac{-2}{\varepsilon^2} - \frac{4}{\varepsilon} + \frac{7\pi^2}{6} - 2 \right) \right]. \quad (2.5)$$

The soft supersymmetry breaking vertex correction

The soft supersymmetry breaking (SSB) vertex correction of diagram Fig. 3(b) possesses neither UV or IR singularities, but it does introduce a dependence on squark and gluino masses. In fact, the effect of this diagram is to multiply the tree level cross section by the finite factor

$$1 + \frac{\alpha_s C_F}{2\pi} \cdot \frac{4A\xi_{\tilde{g}}}{\lambda'} \cdot \Delta_V(\xi_{\tilde{u}}^2, \xi_{\tilde{d}}^2, \xi_{\tilde{g}}^2) \quad (2.6)$$

where, A is the *dimensionful* soft breaking tri-scalar coupling, $\xi_{\tilde{u}} = m_{\tilde{u}}/M$, $\xi_{\tilde{d}} = m_{\tilde{d}}/M$ and $\xi_{\tilde{g}} = m_{\tilde{g}}/M$. The factor $\Delta_V(\xi_{\tilde{u}}^2, \xi_{\tilde{d}}^2, \xi_{\tilde{g}}^2)$ is given by

$$\Delta_V(\xi_{\tilde{u}}^2, \xi_{\tilde{d}}^2, \xi_{\tilde{g}}^2) = \int_0^1 dx \frac{1}{\mu_+(x) + \mu_-(x)} \ln \left[\frac{\mu_-(x)^2 - (\xi_{\tilde{u}}^2 - \xi_{\tilde{d}}^2)^2}{\mu_+(x)^2 - (\xi_{\tilde{u}}^2 - \xi_{\tilde{d}}^2)^2} \right], \quad (2.7)$$

where

$$\mu_{\pm}(x) = \left[x^2 + 2(2\xi_{\tilde{g}}^2 - \xi_{\tilde{u}}^2 - \xi_{\tilde{d}}^2)x + (\xi_{\tilde{u}}^2 - \xi_{\tilde{d}}^2)^2 - 4\xi_{\tilde{g}}^2 \right]^{\frac{1}{2}} \pm x. \quad (2.8)$$

Of course, $\Delta_V(\xi_{\tilde{u}}^2, \xi_{\tilde{d}}^2, \xi_{\tilde{g}}^2)$ may be calculated numerically for any given $\xi_{\tilde{u}}^2$, $\xi_{\tilde{d}}^2$ and $\xi_{\tilde{g}}^2$, but we note that for the case in which the particles are degenerate it can actually be performed

analytically to yield a value of $\pi^2/72$.

The QCD contribution to the quark self-energy

To calculate the contribution from the self energy correction we temporarily shift the external quarks off-shell which enables us to write down a well defined Feynman amplitude for diagrams (c) and (d) in Fig. 3. The one loop self energy kernel ‘ $\Sigma(p)$ ’ has, in addition to the standard QCD contribution, a supersymmetric contribution involving squarks and gluinos. In obvious notation we shall therefore write $\Sigma(p) = \Sigma_{\text{QCD}}(p) + \Sigma_{\text{SUSY}}(p)$. By Lorentz covariance $\Sigma(p)$ must have an expansion in momentum of the form

$$\Sigma(p) = A(p^2) + B(p^2) \not{p}. \quad (2.9)$$

One can easily show that the net effect of including the self energy (SE) correction is to multiply the tree level cross section by the factor

$$1 + 2 \mathcal{R}e B(0), \quad (2.10)$$

where $B(0)$ is (naively) obtained from the self-energy by

$$B(0) = \lim_{p^2 \rightarrow 0} \frac{\partial \Sigma(p)}{\partial \not{p}}. \quad (2.11)$$

The limit in eq. (2.11) must be taken with care since $\Sigma_{\text{QCD}}(p)$ is singular at $p^2 = 0$ when calculated in less than four dimensions. We shall therefore keep $p^2 \neq 0$ until the UV divergences have been renormalized and we have continued to $4 + 2\eta$ dimensions to address the IR divergences. Like the QCD vertex correction $\Sigma_{\text{QCD}}(p)$ is gauge dependent and possesses both UV and IR singularities. The Feynman gauge contribution to the SE from Fig. 5 is

$$\Sigma_{\text{QCD}}(p) = -\frac{\alpha_s C_F}{4\pi} \not{p} \left(\frac{\bar{\mu}^2}{-p^2} \right)^\varepsilon \left(\frac{1}{\varepsilon'} + 1 + O(\varepsilon) \right), \quad (2.12)$$

where the prime on ε indicates a UV pole. Thus, from eq. (2.10) we can see that the effect of the QCD SE correction is to multiply the tree level cross section by the factor

$$1 - \frac{\alpha_s C_F}{2\pi} \left(\frac{\bar{\mu}^2}{-p^2} \right)^\varepsilon \left(\frac{1}{\varepsilon'} + 1 \right) \quad (2.13)$$

which, up to $O(\alpha_s^2, \varepsilon)$ terms, can be written in the desired UV \times IR form

$$\left[1 - \frac{\alpha_s C_F}{2\pi} \left(\frac{\bar{\mu}^2}{M^2} \right)^\varepsilon \frac{1}{\varepsilon'} \right] \left[1 + \frac{\alpha_s C_F}{2\pi} \left(\frac{\bar{\mu}^2}{M^2} \right)^\varepsilon \left(\frac{1}{\varepsilon} - \left(\frac{M^2}{-p^2} \right)^\varepsilon \left(1 + \frac{1}{\varepsilon} \right) \right) \right]. \quad (2.14)$$

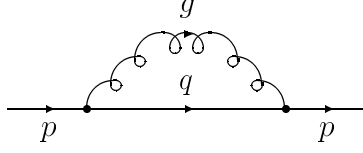


Figure 5: The QCD contribution to the quark self-energy

The supersymmetric contribution to the quark self-energy

The contribution to the self-energy from diagram Fig. 6 is

$$\Sigma_{\text{SUSY}}(p) = -\frac{\alpha_s C_F}{4\pi} \not{p} \left[\left(\frac{\bar{\mu}^2}{M^2} \right)^\epsilon \frac{1}{\epsilon'} - 2 \int_0^1 dx x \ln \left(x(\xi_{\tilde{q}}^2 - \xi_{\tilde{g}}^2) + \xi_{\tilde{g}}^2 \right) \right], \quad (2.15)$$

where \tilde{q} is some generic squark. From eq. (2.10) we can deduce that the effect of the supersymmetric self-energy correction is to simply multiply the tree level cross section by the factor :-

$$1 + \frac{\alpha_s C_F}{2\pi} \left[\Delta_{\text{SE}}(\xi_{\tilde{u}}^2, \xi_{\tilde{d}}^2, \xi_{\tilde{g}}^2) - \left(\frac{\bar{\mu}^2}{M^2} \right)^\epsilon \frac{1}{\epsilon'} \right] \quad (2.16)$$

where the sparticle mass dependent term ' $\Delta_{\text{SE}}(\xi_{\tilde{u}}^2, \xi_{\tilde{d}}^2, \xi_{\tilde{g}}^2)$ ' is given by

$$\Delta_{\text{SE}}(\xi_{\tilde{u}}^2, \xi_{\tilde{d}}^2, \xi_{\tilde{g}}^2) = \int_0^1 dx x \left[\ln \left(x(\xi_{\tilde{u}}^2 - \xi_{\tilde{g}}^2) + \xi_{\tilde{g}}^2 \right) + \ln \left(x(\xi_{\tilde{d}}^2 - \xi_{\tilde{g}}^2) + \xi_{\tilde{g}}^2 \right) \right], \quad (2.17)$$

which can be performed analytically. For a degenerate sparticle mass spectrum we have the trivial result $\Delta_{\text{SE}} = 0$, whilst for the non-degenerate case we find

$$\begin{aligned} \Delta_{\text{SE}}(\xi_{\tilde{u}}^2, \xi_{\tilde{d}}^2, \xi_{\tilde{g}}^2) &= \ln(\xi_{\tilde{u}}\xi_{\tilde{d}}) - \frac{\ln(\xi_{\tilde{u}}/\xi_{\tilde{g}})}{(1 - \xi_{\tilde{u}}^2/\xi_{\tilde{g}}^2)^2} - \frac{\ln(\xi_{\tilde{d}}/\xi_{\tilde{g}})}{(1 - \xi_{\tilde{d}}^2/\xi_{\tilde{g}}^2)^2} \\ &\quad - \frac{1}{2} \left[1 + \frac{1}{1 - \xi_{\tilde{u}}^2/\xi_{\tilde{g}}^2} + \frac{1}{1 - \xi_{\tilde{d}}^2/\xi_{\tilde{g}}^2} \right]. \end{aligned} \quad (2.18)$$

Finally, factoring out the UV pole of (2.16) in the usual manner we find that the multiplicative factor produced by the supersymmetric self-energy correction is

$$\left[1 - \frac{\alpha_s C_F}{2\pi} \left(\frac{\bar{\mu}^2}{M^2} \right)^\epsilon \frac{1}{\epsilon'} \right] \left[1 + \frac{\alpha_s C_F}{2\pi} \Delta_{\text{SE}}(\xi_{\tilde{u}}^2, \xi_{\tilde{d}}^2, \xi_{\tilde{g}}^2) \right] \quad (2.19)$$

Having calculated all the one loop contributions we shall now remove the UV singularities before considering the tree level corrections.

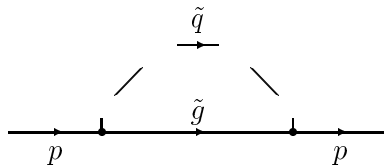


Figure 6: The supersymmetric contribution to the quark self-energy

2.3 Renormalization

It is convenient to make the following choices for L_{UV} and L_{IR} :-

$$L_{UV}\left(\frac{1}{\varepsilon'}\right) = \left(\frac{\bar{\mu}^2}{M^2}\right)^\varepsilon \frac{1}{\varepsilon'} + \frac{1}{2}\Delta_{SE}(\xi_u^2, \xi_d^2, \xi_g^2) + \frac{2A\xi_{\bar{g}}}{\lambda'}\Delta_V(\xi_u^2, \xi_d^2, \xi_g^2), \quad (2.20)$$

$$L_{IR}\left(\frac{1}{\varepsilon}, \frac{1}{\varepsilon'}\right) = \left(\frac{\bar{\mu}^2}{M^2}\right)^\varepsilon \left[\frac{-1}{\varepsilon^2} - \frac{3}{2\varepsilon} + \frac{7\pi^2}{12} - \frac{1}{2}\left(\frac{M^2}{-p^2}\right)^\varepsilon \left(1 + \frac{1}{\varepsilon}\right) - 1 \right]. \quad (2.21)$$

That is, we have chosen to include the finite corrections from the soft SUSY breaking graphs in the UV contribution. To address the problem of renormalization we must identify the renormalization constants Z_1 , Z_2 and Z_3 which are related to each other by

$$Z_1 Z_2 = Z_3 \quad (2.22)$$

and are associated with Yukawa coupling, quark wave-function and Yukawa vertex renormalization respectively. In the $\overline{\text{MS}}$ scheme we find

$$Z_1 = 1 - \frac{\alpha_s C_F}{2\pi} \frac{1}{\hat{\varepsilon}}, \quad Z_2 = 1 - \frac{\alpha_s C_F}{2\pi} \frac{1}{\hat{\varepsilon}}, \quad Z_3 = 1 - \frac{\alpha_s C_F}{\pi} \frac{1}{\hat{\varepsilon}}, \quad (2.23)$$

where

$$\frac{1}{\hat{\varepsilon}} = \frac{1}{\varepsilon} + \ln 4\pi - \gamma_E. \quad (2.24)$$

As one would expect the renormalization constants Z_2 and Z_3 are gauge dependent but Z_1 , pertaining to a physical observable, is gauge invariant. Calculation of the QCD loop diagrams in Landau gauge (see Appendix) leads us to conclude Z_2 and Z_3 to be

$$Z_2 = 1 - \frac{\alpha_s C_F}{4\pi} \frac{1}{\hat{\varepsilon}}, \quad Z_3 = 1 - \frac{\alpha_s C_F}{4\pi} \frac{3}{\hat{\varepsilon}}. \quad (2.25)$$

Thus, we can deduce that in a general R_ξ gauge

$$Z_2 = 1 - \frac{\alpha_s C_F}{\pi} \left(\frac{\xi + 1}{4}\right) \frac{1}{\hat{\varepsilon}}, \quad Z_3 = 1 - \frac{\alpha_s C_F}{\pi} \left(\frac{\xi + 3}{4}\right) \frac{1}{\hat{\varepsilon}}. \quad (2.26)$$

from which one can see Z_1 is still given by the gauge invariant expression in eq. (2.23). Having determined Z_1 one finds that the $O(\alpha_s)$ beta function for the R_p -breaking coupling λ' is

$$\beta_{\lambda'} = \mu \frac{d\lambda'}{d\mu} = -\lambda' \frac{\alpha_s C_F}{\pi}, \quad (2.27)$$

which clearly shows that λ' decreases as the scale μ is increased. Solving eq. (2.27) we find

$$\lambda'(M^2) = \lambda'(\mu^2) \left[1 + \frac{\alpha_s C_F}{2\pi} \ln \left(\frac{\mu^2}{M^2} \right) \right] + O(\alpha_s^2). \quad (2.28)$$

Before moving on to consider the resultant renormalized contribution to the cross section, we note that by performing an additional finite renormalization on λ' we can ‘remove’ the residual finite terms in eq. (2.20). In all subsequent work we shall assume that this finite renormalization has been performed.

Adding the contributions from the renormalized loop graphs to the leading tree level graph we find the resultant to be

$$K_0(M^2) \left(1 + \frac{\alpha_s C_F}{\pi} L_{\text{IR}} \left(\frac{1}{\varepsilon}, \frac{1}{\varepsilon^2} \right) \right) \quad (2.29)$$

where the ‘running’ tree level cross section is

$$K_0(M^2) = \frac{2^{-\varepsilon} \pi \lambda'^2(M^2)}{12S}. \quad (2.30)$$

Thus, the net effect of the UV renormalization is to simply replace the scale independent Yukawa coupling λ' by a running coupling $\lambda'(M^2)$ whose evolution is governed by eq. (2.28). Since the UV renormalization procedure is now complete, we can now continue from $4 - 2\varepsilon$ dimensions to $4 + 2\eta$ (with $\eta > 0$) dimensions to regularise the IR divergences. In $4 + 2\eta$ dimensions we can safely take the $p^2 \rightarrow 0$ limit of L_{IR} in eq. (2.21) and obtain the well defined result

$$L_{\text{IR}} \left(\frac{1}{\eta}, \frac{1}{\eta^2} \right) = \left(\frac{M^2}{\bar{\mu}^2} \right)^\eta \left[-\frac{1}{\eta^2} + \frac{3}{2\eta} + \frac{7\pi^2}{12} - 1 \right]. \quad (2.31)$$

2.4 The NLO tree level contribution

The two body phase space (in 2ω dimensions) for the on-shell particle pair production diagrams in Fig. 4 is (*c.f.* [4])

$$d\Phi_{(2)} = \frac{d^{2\omega} p_3}{(2\pi)^{2\omega}} \frac{d^{2\omega} p_4}{(2\pi)^{2\omega}} \cdot (2\pi)^{2\omega} \delta(p_1 + p_2 - p_3 - p_4) \cdot 2\pi \delta^+(p_3^2 - M^2) \cdot 2\pi \delta^+(p_4^2), \quad (2.32)$$

where (p_1, p_2) and (p_3, p_4) denote the momenta of the incoming and outgoing particles respectively, with p_3 being the momentum of the slepton. The partonic Mandelstam variables (s, t, u) are defined in the usual way by

$$s = (p_1 + p_2)^2, \quad t = (p_1 - p_3)^2, \quad u = (p_1 - p_4)^2, \quad (2.33)$$

and in terms of $w = \frac{1}{2}(1 + \hat{\mathbf{p}}_4 \cdot \hat{\mathbf{p}}_2)$ and $z = M^2/s$ we find t and u are

$$t = -\frac{M^2}{z}(1-z)(1-w), \quad u = -\frac{M^2}{z}(1-z)w. \quad (2.34)$$

Using these identities to write the differential phase space in terms of z and w we find after some simple algebra

$$\frac{d\Phi_{(2)}}{dw} = \frac{1}{8\pi\Gamma(\omega-1)} \left(\frac{M^2}{4\pi}\right)^{\omega-2} (1-z) \left[\frac{(1-z)^2}{z}\right]^{\omega-2} (w(1-w))^{\omega-2}. \quad (2.35)$$

Setting $\eta = \omega - 2$ and using the result[5]

$$\Gamma(1+\xi) = \exp\left(-\gamma_E\xi + \frac{\pi^2}{12}\xi^2\right) + O(\xi^3) \quad (2.36)$$

we find eq. (2.35) becomes

$$\frac{d\Phi_{(2)}}{dw} = \frac{(\mu^2)^\eta}{8\pi} \left(\frac{M^2}{\bar{\mu}^2}\right)^\eta \frac{(1-z)^{1+2\eta}}{z^\eta} \left(1 - \frac{\pi^2}{12}\eta^2\right) (w(1-w))^\eta + O(\eta^3), \quad (2.37)$$

where we have explicitly introduced an arbitrary mass scale ‘ μ ’. Thus, contribution to the elementary cross section (in $4 + 2\eta$ dimensions) from any one of the diagrams in Fig. 4 has the form

$$\hat{\sigma} = \frac{(\mu^2)^\eta}{16\pi s} \left(\frac{M^2}{\bar{\mu}^2}\right)^\eta \frac{(1-z)^{1+2\eta}}{z^\eta} \left(1 - \frac{\pi^2}{12}\eta^2\right) \int_0^1 dw (w(1-w))^\eta \langle |\mathcal{M}(z, w)|^2 \rangle_{(\eta)} + O(\eta), \quad (2.38)$$

where $\langle |\mathcal{M}(z, w)|^2 \rangle_{(\eta)}$ denotes the appropriate (spin/colour averaged) squared Feynman amplitude in $4 + 2\eta$ dimensions.

Turning our attention to the ‘gluon-bremsstrahlung’ diagrams in Fig. 4(a), (b) we find after a brief calculation

$$\langle |\mathcal{M}_a + \mathcal{M}_b|^2 \rangle = 16\pi S K_0(M^2) \frac{g^2 C_F}{8\pi^2} \left[\frac{(s-M^2)^2}{ut} (1+\eta) + \frac{2sM^2}{ut} \right]. \quad (2.39)$$

In terms of w and z eq. (2.39) becomes

$$\langle |\mathcal{M}_a + \mathcal{M}_b|^2 \rangle = \frac{16\pi S K_0(M^2) g^2 C_F}{w(1-w) 8\pi^2} \left[\frac{1+z^2}{(1-z)^2} + \eta \right], \quad (2.40)$$

and so from eq. (2.38) we find that the contribution of the gluon bremsstrahlung diagrams to the elementary cross section is

$$K_0(M^2) \frac{S}{s} \frac{\alpha_s C_F}{2\pi} \left(\frac{M^2}{\bar{\mu}^2}\right)^\eta \frac{(1-z)^{1+2\eta}}{z^\eta} \left(1 - \frac{\pi^2}{12}\eta^2\right) \left[\frac{1+z^2}{(1-z)^2} + \eta \right] I(\eta) + O(\eta), \quad (2.41)$$

where

$$I(\eta) = \int_0^1 dw (w(1-w))^{\eta-1}. \quad (2.42)$$

This integral can be calculated directly in terms of the Euler Beta function:

$$I(\eta) = B(\eta, \eta) = \frac{2}{\eta} - \frac{\pi^2}{3}\eta + O(\eta^2), \quad (2.43)$$

where we have used eq. (2.36) to obtain the power series expansion. With this result (2.41) becomes

$$K_0(M^2) \frac{S}{s} \frac{\alpha_s C_F}{\pi} \left(\frac{M^2}{\bar{\mu}^2} \right)^\eta \left(1 - \frac{\pi^2}{4}\eta^2 \right) \left[\frac{z^{-\eta}}{\eta} (1+z^2)(1-z)^{-1+2\eta} + z^{-\eta} (1-z)^{1+2\eta} \right] + O(\eta). \quad (2.44)$$

After isolating the soft gluon pole at $z = 1$ and performing a power series expansion in η , we find the content of the square bracket in eq. (2.44) is

$$\frac{1}{\eta^2} \delta(1-z) + \frac{1}{\eta} \frac{1+z^2}{(1-z)_+} + (1+z^2) \left(\frac{\ln(1-z)^2}{1-z} \right)_+ - (1+z^2) \frac{\ln z}{1-z} + 1 - z + O(\eta), \quad (2.45)$$

where the ‘+’ indicates conventional distributional regularisation on $[0, 1]$. Upon addition of the contributions from the gluon-bremsstrahlung diagrams and the loop diagrams (which have support only at $z = 1$) the double poles cancel and the resulting contribution ‘ $\Delta \hat{\sigma}$ ’ to the elementary cross section is

$$\Delta \hat{\sigma} = K_0(M^2) \frac{S}{s} \left[\delta(1-z) + \frac{\alpha_s C_F}{2\pi} \left(2 P_{qq}(z) \ln \left(\frac{M^2}{\mu^2} \right) + A(z) \right) \right] + O(\alpha_s^2), \quad (2.46)$$

where

$$P_{qq}(z) = \frac{1+z^2}{(1-z)_+} + \frac{3}{2} \delta(1-z), \quad (2.47)$$

is the quark \rightarrow quark ‘splitting function’, and

$$\begin{aligned} A(z) &= 2 \left(\frac{1}{\eta} - \ln 4\pi + \gamma_E \right) P_{qq}(z) + \left(\frac{2\pi^2}{3} - 2 \right) \delta(1-z) + 2(1-z) \\ &\quad + 2(1+z^2) \left(\frac{\ln(1-z)^2}{1-z} \right)_+ - 2(1+z^2) \frac{\ln z}{1-z}. \end{aligned} \quad (2.48)$$

We now turn our attention to the ‘Compton’ like graphs in Fig. 4(c),(d). The contribution from these graphs is obtained from eq. (2.39) by making the replacement $s \leftrightarrow -u$. Thus,

$$\langle |\mathcal{M}_c + \mathcal{M}_d|^2 \rangle = -16\pi S K_0(M^2) \frac{g^2 T_F}{8\pi^2} \left[\frac{(u-M^2)^2}{st} (1+\eta) + \frac{2uM^2}{st} \right], \quad (2.49)$$

where

$$T_F \delta^{ab} = \text{tr}(T^a T^b) = \frac{1}{2} \delta^{ab} \quad (2.50)$$

is the quadratic trace in the fundamental representation. In terms of w and z the RHS of eq. (2.49) becomes

$$16\pi S K_0(M^2) \frac{g^2 T_F}{8\pi^2} \left[\frac{z^2}{(1-w)(1-z)} + (1-z) \frac{w^2}{(1-w)} + \eta \frac{[z + (1-z)w]^2}{(1-w)(1-z)} \right]. \quad (2.51)$$

Thus, the contribution to the elementary cross section is

$$K_0(M^2) \frac{S}{s} \frac{\alpha_s T_F}{2\pi} \left(\frac{M^2}{\bar{\mu}^2} \right)^\eta \frac{(1-z)^{1+2\eta}}{z^\eta} \left(1 - \frac{\pi^2}{12} \eta^2 \right) I(z, \eta), \quad (2.52)$$

where

$$I(z, \eta) = \int_0^1 dw (w(1-w))^\eta \left[\frac{z^2}{(1-w)(1-z)} + (1-z) \frac{w^2}{(1-w)} + \eta \frac{[z + (1-z)w]^2}{(1-w)(1-z)} \right]. \quad (2.53)$$

Using eq. (2.36) to expand the Euler Beta functions which arise from the above integrals we obtain

$$I(z, \eta) = \frac{z^2}{1-z} \left(\frac{1}{\eta} + 1 \right) + (1-z) \left(\frac{1}{\eta} - \frac{1}{2} \right) + 2z + O(\eta). \quad (2.54)$$

Expanding the remaining terms of (2.52) as a power series in η we find that the $O(\alpha_s)$ contribution of the Compton type diagrams to the elementary cross section is

$$K_0(M^2) \frac{S}{s} \frac{\alpha_s T_F}{2\pi} \left[P_{qg}(z) \ln \left(\frac{M^2}{\mu^2} \right) + B(z) \right] + O(\eta), \quad (2.55)$$

where

$$P_{qg}(z) = z^2 + (1-z)^2 \quad (2.56)$$

is the gluon \rightarrow quark ‘splitting function’, and

$$B(z) = \left(\frac{1}{\eta} - \ln 4\pi + \gamma_E \right) P_{qg}(z) + P_{qg}(z) \ln \frac{(1-z)^2}{z} - \frac{3}{2} z^2 + 3z - \frac{1}{2}. \quad (2.57)$$

Denoting the appropriate product of quark and gluon densities by $K(x_1, x_2)$:-

$$K(x_1, x_2) = (u(x_1) + \bar{d}(x_1))g(x_2) + (u(x_2) + \bar{d}(x_2))g(x_1), \quad (2.58)$$

we can now write down the total $O(\alpha_s)$ hadronic cross section

$$\begin{aligned}\sigma_H &= K_0(M^2) \int \frac{dx_1}{x_1} \frac{dx_2}{x_2} H(x_1, x_2) \left[\delta(1-z) + \theta(1-z) \frac{\alpha_s C_F}{2\pi} \left(2 P_{qq}(z) \ln \left(\frac{M^2}{\mu^2} \right) + A(z) \right) \right] \\ &+ K_0(M^2) \int \frac{dx_1}{x_1} \frac{dx_2}{x_2} K(x_1, x_2) \theta(1-z) \frac{\alpha_s T_F}{2\pi} \left[P_{qg}(z) \ln \left(\frac{M^2}{\mu^2} \right) + B(z) \right].\end{aligned}\quad (2.59)$$

Expressing the ‘bare’ quark densities in terms of their scale dependent ‘renormalised’ counterparts we have

$$\begin{aligned}q(x) &= q(x, Q^2) - \frac{\alpha_s C_F}{2\pi} \int_x^1 \frac{dz}{z} \left(P_{qq}(z) \ln \left(\frac{Q^2}{\mu^2} \right) + f_q(z) \right) q(x/z, Q^2) \\ &- \frac{\alpha_s T_F}{2\pi} \int_x^1 \frac{dz}{z} \left(P_{qg}(z) \ln \left(\frac{Q^2}{\mu^2} \right) + f_g(z) \right) g(x/z, Q^2) + O(\alpha_s^2),\end{aligned}\quad (2.60)$$

where in the $\overline{\text{MS}}$ factorisation scheme[4]

$$\begin{aligned}f_q(z) &= \left(\frac{1}{\eta} - \ln 4\pi + \gamma_E \right) P_{qq}(z) + (1+z^2) \left(\frac{\ln(1-z)}{1-z} \right)_+ - \frac{3}{2} \frac{1}{(1-z)_+} \\ &- \left(\frac{9}{2} + \frac{1}{3}\pi^2 \right) \delta(1-z) - (1+z^2) \frac{\ln z}{1-z} + 3 + 2z,\end{aligned}\quad (2.61)$$

$$f_g(z) = \left(\frac{1}{\eta} - \ln 4\pi + \gamma_E \right) P_{qg}(z) + P_{qg}(z) \ln \frac{1-z}{z} + 6z(1-z).\quad (2.62)$$

Thus, with the removal of all bare parton densities we obtain our result for the NLO hadronic cross section:

$$\begin{aligned}\sigma_H &= K_0(M^2) \int \frac{dx_1}{x_1} \frac{dx_2}{x_2} H(x_1, x_2; M^2) \left[\delta(1-z) + \theta(1-z) \frac{\alpha_s C_F}{2\pi} 2 F^{(T)}(z) \right] \\ &+ K_0(M^2) \int \frac{dx_1}{x_1} \frac{dx_2}{x_2} K(x_1, x_2; M^2) \theta(1-z) \frac{\alpha_s T_F}{2\pi} G^{(T)}(z) + O(\alpha_s^2),\end{aligned}\quad (2.63)$$

where $F^{(T)}(z) = \frac{1}{2}A(z) - f_q(z)$ and $G^{(T)}(z) = B(z) - f_g(z)$ have the explicit forms

$$\begin{aligned}F^{(T)}(z) &= \frac{3}{2} \frac{1}{(1-z)_+} + (1+z^2) \left(\frac{\ln(1-z)}{1-z} \right)_+ - 2 - 3z \\ &+ \left(\frac{2}{3}\pi^2 + \frac{7}{2} \right) \delta(1-z),\end{aligned}\quad (2.64)$$

$$G^{(T)}(z) = (z^2 + (1-z)^2) \ln(1-z) + \frac{9}{2} z^2 - 3z - \frac{1}{2}.\quad (2.65)$$

One caveat in extracting numerical results from eq. (2.63) is that the renormalization scale of α_s remains undetermined in our $O(\alpha_s)$ calculation. Of course, this result could have

been anticipated from the RGE for α_s :-

$$\frac{d\alpha_s}{dt} \sim \alpha_s^2, \quad (2.66)$$

where $\alpha_s^2 = 0$ to the level of approximation in this calculation. In order to obtain numerical results one must assume a scale for α_s and our choice, although not rigorously justifiable without including $O(\alpha_s^2)$ corrections, was the slepton mass ‘ M ’. The consequence of choosing the the scale of α_s to be S rather than M is simply to shift the cross section by terms of order α_s^2 . We evaluated the NLO hadronic cross section (at $\sqrt{S} = 14$ TeV) with several recent structure function sets using the PDFLIB package[6]. Our principal result in Fig. 7 shows the NLO hadronic cross section calculated using the GRV HO set[7] as a function of slepton mass ranging from 100 GeV to 10 TeV.

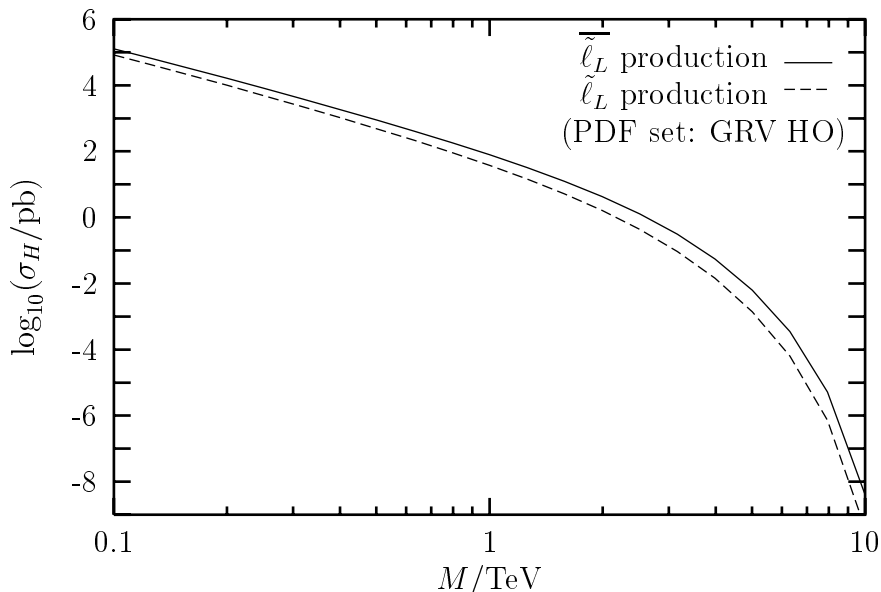


Figure 7: The NLO hadronic cross section for $\lambda'_{i11} = 1$

Fig. 8 shows the magnitude of NLO cross sections calculated using three different PDF sets² (namely, CTEQ 2pM[8], MRS (H)[9] and MRS D'_-[10]) relative to the one in Fig. 7. In Fig. 9 we show the ratio of the NLO to tree level cross sections using all four PDFs. The fact that this ratio increases with slepton mass simply means that the NLO cross section falls off more slowly than the tree level cross section. As one can see the corrections are quite significant, especially for slepton masses in excess of $O(1)$ TeV.

²All of the PDF sets used are NLL evolutions calculated in the $\overline{\text{MS}}$ factorisation scheme and are consistent with current low- x data.

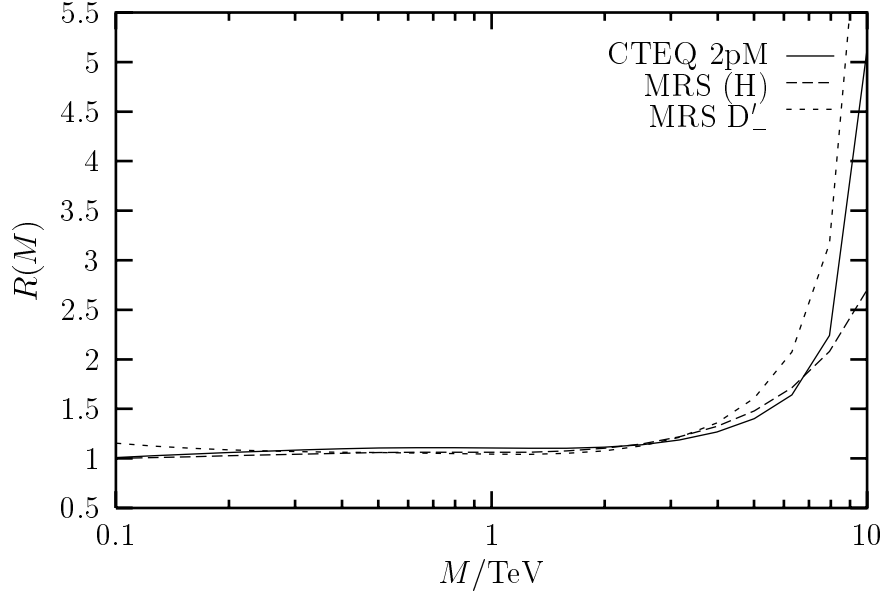


Figure 8: $R(M) = \sigma_H^{(i)} / \sigma_H^{(\text{GRV HO})}$; $i = \text{CTEQ 2pM, MRS (H), MRS D'}$

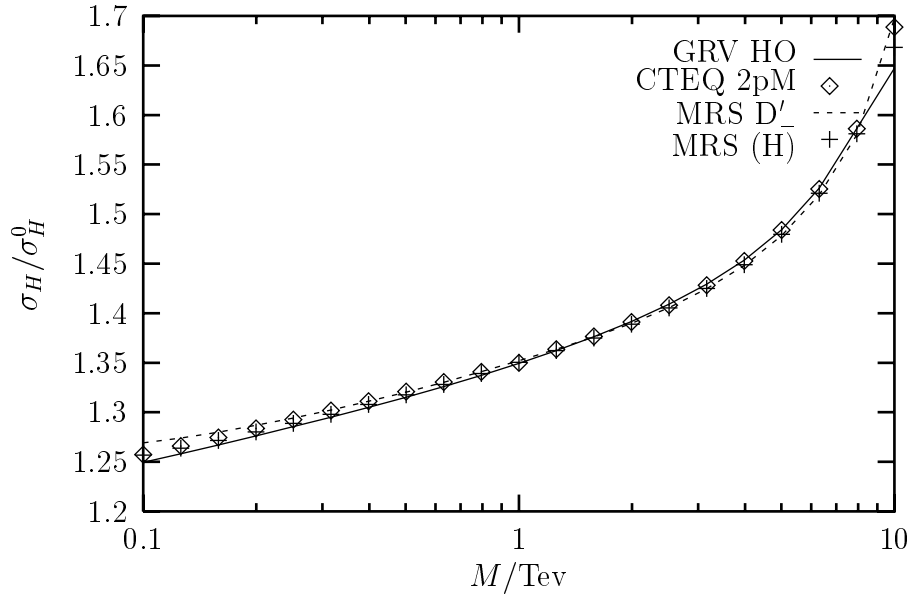


Figure 9: Ratio of NLO to tree level cross sections

Finally, we use the results displayed in Fig. 7 to determine the critical coupling (λ'_c) for ‘discovery’ at the LHC. Our results in Fig. 10 are based on a sample size of 10^5 pb^{-1} , (comparable to one year’s worth of data) and assume a discovery at 95%CL. The experimental bounds[11] on λ'_{111} , and λ'_{211} (λ'_{311} is currently unbounded) are plotted³ for comparison on the same graph. As one can see, even in the worst case, there is a window for discovery for $M \leq O(6) \text{ TeV}$.

³These bounds are valid if one assumes that the squarks and sleptons are degenerate

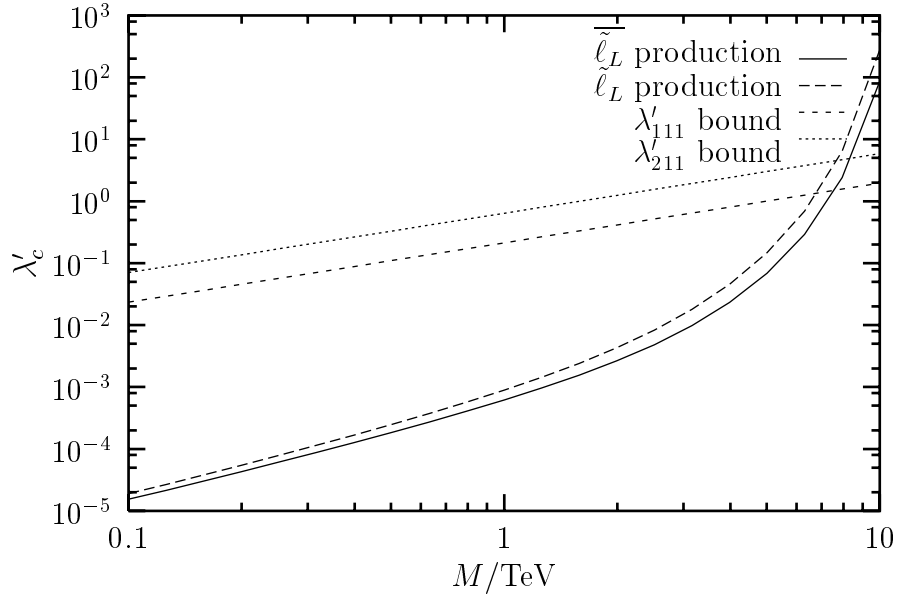


Figure 10: Critical coupling for discovery in 10^5 pb^{-1} of data

3 Conclusion

We have calculated the NLO hadronic cross section for monoslepton at the LHC and have shown that the leading QCD corrections are potentially large. Depending on the ratio $\rho = m_{\tilde{\gamma}}/m_{\tilde{\ell}}$ the optimal signal for monoslepton production interpolates between a hard isolated lepton with energy $O(m_{\tilde{\ell}}/2)$ recoiling against a jet when $\rho \ll 1$, and an isolated like-sign dilepton for $\rho \lesssim 1$. Potential backgrounds from $t \rightarrow bW^+$ or $q\bar{q}$, $H^0 \rightarrow W^+W^-$ can be excluded by suitable energy cuts or by event topology.

Acknowledgements

I would like to thank P. L. White and S. F. King for useful comments.

Appendix: QCD corrections in Landau gauge

We now briefly present summarised results of a Landau gauge calculation of the one loop QCD corrections. In this gauge we find that the one loop QCD self energy correction vanishes[12]:

$$\Sigma_{\text{QCD}}(p) = 0. \quad (\text{A1})$$

Consequently, the only non-trivial contribution to $\Sigma(p)$ is from $\Sigma_{\text{SUSY}}(p)$:-

$$\Sigma(p) = -\frac{\alpha_s C_F}{4\pi} \not{p} \left[\left(\frac{\bar{\mu}^2}{M^2} \right)^\varepsilon \frac{1}{\varepsilon'} - 2 \int_0^1 dx x \ln \left(x(\xi_{\bar{q}}^2 - \xi_{\bar{g}}^2) + \xi_{\bar{g}}^2 \right) \right]. \quad (\text{A2})$$

The resultant effect of the Landau gauge self-energy corrections is to multiply the tree level cross section by the overall factor

$$\left[1 - \frac{\alpha_s C_F}{2\pi} \left(\frac{\bar{\mu}^2}{M^2} \right)^\varepsilon \frac{1}{\varepsilon'} \right] \left[1 + \frac{\alpha_s C_F}{2\pi} \Delta_{\text{SE}}(\xi_{\bar{u}}^2, \xi_{\bar{d}}^2, \xi_{\bar{g}}^2) \right], \quad (\text{A3})$$

where $\Delta_{\text{SE}}(\xi_{\bar{u}}^2, \xi_{\bar{d}}^2, \xi_{\bar{g}}^2)$ is given in eq. (2.18). Turning our attention to the vertex correction we find the contribution from the one loop QCD diagram in Landau gauge is the multiplicative factor (c.f. eq. (2.5)):-

$$\left[1 + \frac{\alpha_s C_F}{2\pi} \left(\frac{\bar{\mu}^2}{M^2} \right)^\varepsilon \frac{3}{\varepsilon'} \right] \left[1 + \frac{\alpha_s C_F}{2\pi} \left(\frac{\bar{\mu}^2}{M^2} \right)^\varepsilon \left(-\frac{2}{\varepsilon^2} - \frac{3}{\varepsilon} + \frac{7\pi^2}{6} - 2 \right) \right] + O(\alpha_s^2, \varepsilon). \quad (\text{A4})$$

We now find the renormalization constants Z_2 and Z_3 to be

$$Z_2 = 1 - \frac{\alpha_s C_F}{4\pi} \frac{1}{\hat{\varepsilon}}, \quad Z_3 = 1 - \frac{\alpha_s C_F}{4\pi} \frac{3}{\hat{\varepsilon}}, \quad (\text{A5})$$

and subsequently the Yukawa coupling renormalization constant Z_1 is

$$Z_1 = \frac{Z_3}{Z_2} = 1 - \frac{\alpha_s C_F}{2\pi} \frac{1}{\hat{\varepsilon}} \quad (\text{A6})$$

which, as expected, is identical to the result obtained in the Feynman gauge.

References

- [1] M. Bento, L. J. Hall and G. G. Ross, Nucl. Phys. B292 (1987) 400.
- [2] L. J. Hall and M. Suzuki, Nucl. Phys. B231 (1984) 419.
- [3] H. Dreiner and G. G. Ross, Oxford university preprint OUTP-91-15P (1991); S. Lola and J. McCurry, Nucl. Phys. B381 (1992) 559-576; J. Butterworth and H. Dreiner, Nucl. Phys. Nucl. Phys. B397 (1993) 3-34.
- [4] G. Altarelli, R. K. Ellis and G. Martinelli, Nucl. Phys. B157 (1979) 461-497.

- [5] M. Abramowitz and I. A. Stegun, Handbook of Mathematical Functions (9/e) (Dover Publ., 1970) p.1005.
- [6] H. Plathow-Besch, Comp. Phys. Comm. 75 (1993) 396-416; H. Plathow-Besch, PDFLIB: Nucleon, Pion, and Photon Parton Density Functions and α_s Calculations (User's Manual - Version 4.16, W5051, PDFLIB, 1994.01.11, CERN-PPE).
- [7] M. Glück, E. Reya and A. Vogt, Z. Phys. C53 (1992) 127 and Phys. Lett. 306B (1993) 391.
- [8] CTEQ Collaboration, J. Botts *et al.*, to be published.
- [9] A. D. Martin, R. G. Roberts and W. J. Stirling, RAL preprint, RAL-93-077 (1993).
- [10] A. D. Martin, R. G. Roberts and W. J. Stirling, Phys. Lett, 306B (1993) 145 (E: Phys. Lett. 309B (1993) 492).
- [11] V. Barger, G. F. Giudice, T. Han, Phys. Rev. D40 (1989) 2987.
- [12] W. J. Marciano, Phys. Rev. D12 (1975) 3861.